Design, production, and reverse engineering of two-octave antireflection coatings

Tatiana V. Amotchkina,[1,*] Michael K. Trubetskov,[1] Vladimir Pervak,[2] and Alexander V. Tikhonravov[1]

[1]Research Computing Center, Moscow State University, Leninskie Gory, 119991, Moscow, Russia

[2]Ludwig-Maximilians-Universitaet München, Am Coulombwall 1, D-85748 Garching, Germany

*Corresponding author: tatiana@srcc.msu.ru

Received 22 July 2011; revised 31 August 2011; accepted 31 August 2011; posted 7 September 2011 (Doc. ID 151587); published 2 December 2011

We deal with design and production of optimal two-component antireflection (AR) coatings for an ultra broadband spectral range from 450 nm to 1800 nm. We demonstrate the whole design-production chain including design selection, choosing monitoring technique, coating production, and reverse engineering of the deposited coatings. At each step of this chain we provide thorough analysis on the basis of theoretical results and adequate computational manufacturing experiments. In order to produce the designed AR coatings we use magnetron sputtering deposition technique and accurate time monitoring. © 2011 Optical Society of America

OCIS codes: 310.1210, 310.1860, 310.4165, 310.5696, 310.6805.

1. Introduction

Antireflection (AR) coatings is the most widely used type of optical interference coatings. They form more than 50% of total optical coatings market [1]. It is not surprising, therefore, that a great number of papers and several books devoted to AR have been published. The list of the most essential publications in the field of AR and chronological reviews of AR design techniques can be found in [2–11]. In the last several years the activity of researchers, dealing with various theoretical and experimental aspects of AR coatings, continually grows. Recently, we published a series of papers [10,12–14] where we performed a comprehensive theoretical research on broadband AR designs. We provided a definition of an optimal AR design, confirmed cluster structure of optimal AR designs, obtained estimations for the number of layers in such designs, found a dependence of AR average residual reflectance on design total optical thickness (TOT). We demonstrated also that there exists a minimal nonzero achievable residual reflectance and derived an accurate empirical expression for this value [10,14].

The authors of [1] provided a well-grounded complete study aimed at design, analysis, and production of AR for the visible spectral range. It was demonstrated in [1] that computational simulation of a deposition process and a monitoring algorithm are of great importance for design selection and production yield estimations. The experimental results obtained by these authors demonstrate high stability of the designed AR.

Experimental and theoretical results on design and production of the AR coatings for the spectral range from 400 nm to 1200 nm were reported [15]. In [15] AR coatings with a specially structured last layer were produced and benefits in performance of such coatings in comparison with conventional two-component multilayer AR designs were demonstrated.

The main goal of our present study is to design and produce optimal AR coatings working in an ultra broadband spectral range with the ratio of the upper wavelength and the lower wavelength limits equal to four. As opposed to [15], our goal is to produce conventional two-component multilayer AR coatings. Production of high quality broadband AR coatings

0003-6935/11/356468-08$15.00/0
© 2011 Optical Society of America

satisfying a specified requirement on performance is not a straightforward task mainly because optimal AR designs contain layers with thickness less than 10 nm. Controlling such layers can be a problem in the course of a deposition process. We intentionally do not modify the design structure in order to avoid thin layers. We demonstrate that the production of optimal AR designs in their original form is realistic, when a broadband AR coating is produced with a stable deposition process controlled by an appropriate accurate monitoring technique.

In our recent papers [16–18] we demonstrated that the selection of a design affects a monitoring technique to be used in the course of its deposition. We proposed also a procedure for monitoring technique selection and production yield estimation on the basis of computational manufacturing experiments [18,19]. In the present study we have two monitoring techniques at our disposal, namely broadband optical monitoring and time monitoring. To choose the monitoring technique suitable for AR coating deposition we perform computational manufacturing experiments simulating production runs controlled by these two techniques. Applying our previous results [16,18] we establish that, in the case of the considered AR designs, a time monitoring technique is preferable. To produce AR designs we use magnetron sputtering which is considered as a stable deposition process. Therefore we expect neither wavelength shift upon venting nor any temperature shift.

In order to demonstrate adequacy of our computational manufacturing experiments and confirm the results of these experiments, determination of deposition errors in produced AR coatings is required. We perform reverse engineering of the produced AR coatings on the basis of transmittance data measured *in situ* [20]. Therefore, in general we propose the whole design-production chain starting from design selection and finishing with reverse engineering of the deposited AR coatings.

In Section 2 we describe our design procedure and select AR designs for production purpose. In Section 3 we choose an appropriate monitoring technique on the basis of computational manufacturing experiments. In Section 4 we describe our deposition process and available measurement data. Also in this section we compare measured and theoretical transmittance data related to AR samples. In Section 5 we determine errors in layer parameters made in the course of the deposition process and confirm evidence of validity of our preliminary computational manufacturing procedures. Our conclusions are presented in Section 6.

2. Selection of Two-Octave AR Designs

In this section we select AR designs for the spectral range from $\lambda_l = 450$ nm to $\lambda_u = 1800$ nm, i.e. $\lambda_u/\lambda_l = 4$. Optical coatings working in spectral ranges of such width are called two-octave coatings.

In this paper we design and produce multilayer AR coatings on the basis of two pairs of high and low index materials, namely Ta_2O_5/SiO_2 and Nb_2O_5/SiO_2. We reduce the reflection of the 6.35 mm thick Suprasil substrates for the normal incidence case. Refractive index wavelength dependencies of thin-film materials are described by a well-known Cauchy formula:

$$n(\lambda) = A_0 + A_1(\lambda_0/\lambda)^2 + A_2(\lambda_0/\lambda)^4, \qquad (1)$$

where A_0, A_1, and A_2 are dimensionless parameters, $\lambda_0 = 1000$ nm, wavelength λ is specified in nanometers. The values of Cauchy parameters of thin-film materials are presented in the first three rows of Table 1. Dispersion data of Suprasil substrate are taken from Heraeus Quartzglas catalog [21].

The average residual reflectance R_{av} of an AR design is defined as [10,14]

$$R_{av} = \frac{1}{\lambda_u - \lambda_l} \int_{\lambda_l}^{\lambda_u} R(\lambda) d\lambda, \qquad (2)$$

where $R(\lambda)$ is the spectral reflectance of the AR design under consideration.

It is known that TOT is a key design parameter [10,22] and the definition of an optimal design is tightly connected with TOT. A design is an optimal AR if it provides a minimum value of R_{av} among all possible designs with TOTs close to a specified TOT value [23].

It was shown in [4,10,12] that optimal AR designs consist of quasi-periodic groups of layers, so-called clusters. A semiempirical expression for the number of layers in one-cluster N_c was derived in [13]

$$N_c = 2\left(\left[\frac{\lambda_c}{\lambda_l}\right] + 1\right),$$
$$\lambda_c = \lambda_u \left\{1 + \frac{2}{\pi} \arcsin\left(\frac{n_H/n_L - 1}{n_H/n_L + 1}\right)\right\}. \qquad (3)$$

Optical thickness of one-cluster T_c was estimated in [4]

$$T_c = \frac{\lambda_u}{2}\left[1 + \frac{2}{\pi} \arcsin\left(\frac{n_H/n_L - 1}{n_H/n_L + 1}\right)\right]. \qquad (4)$$

In order to estimate N_c and T_c values for our AR design problems we substitute in Eqs. (3) and (4) n_H and n_L values calculated by Cauchy formula (1) at a central wavelength point $(\lambda_u \lambda_l)^{1/2} = 900$ nm of the antireflection spectral range. In the case of Ta_2O_5/SiO_2 AR we obtain $n_H = 2.09$, in the case of Nb_2O_5/SiO_2 design we have $n_H = 2.25$, and in both

Table 1. Cauchy Parameters of Thin-Film Materials and Substrates

Material	A_0	A_1	A_2
Ta_2O_5	2.065721	0.01683	0.001686
Nb_2O_5	2.218485	0.021827	$3.99968 \cdot 10^{-3}$
SiO_2	1.460472	0	$4.9867 \cdot 10^{-4}$
Glass	1.500859	$3.26477 \cdot 10^{-3}$	$5.0404 \cdot 10^{-4}$

cases $n_L = 1.46$. The estimated value of N_c equals to 10 in both cases and T_c values equal to 1002 nm and 1023 nm in the case of Ta_2O_5/SiO_2 and Nb_2O_5/SiO_2, respectively. These estimations indicate that to improve AR design performance, approximately 10 layers are to be added and coating optical thickness is to be increased by about 1 μm.

In our design we are interested in achieving a good performance of AR, on the one hand, and in practical feasibility of the design, on the other hand. Adding new clusters to AR designs reduces its average residual reflectance but at the same time the number of layers grows and the design structure becomes more complicated. In this case a compromised solution should be found. This compromise should provide acceptable R_{av} values as well as relatively small number of layers. Searching for this solution we base on the estimation of relative decrease of R_{av}. This decrease can be achieved when we add a new cluster [10]. It was recommended in [10] not to consider AR designs having more than 2–3 clusters because the relative decrease of R_{av} becomes negligible and R_{av} is already approaching to the minimal achievable residual reflectance R_∞. In the present work we limit ourselves by considering AR designs consisting of one, two, and three clusters.

Our AR design process is based on the minimization of average residual reflectance written in the numerical form

$$R_{av} = \frac{1}{L}\sum_{j=1}^{L} R(\lambda_j), \quad (5)$$

where $L = 676$ (large enough for two-octave AR) and $\{\lambda_j\}$, $j = 1, \ldots, L$ is a logarithmic grid in the AR spectral range defined by a formula:

$$\lambda_j = \lambda_l r^{j-1}, \qquad r = \exp\left[\frac{\ln(\lambda_u/\lambda_l)}{L-1}\right], \qquad j = 1 \ldots, L. \quad (6)$$

The logarithmic grid provides distribution of spectral points that is more dense in the short wavelength region and more sparse in the long wavelength region. In many cases, including broadband AR problems, using a logarithmic grid allows one to obtain better results than using a uniform wavenumber grid.

In the course of the design process we use a needle optimization technique incorporated in OptiLayer thin-film software [24]. We start needle optimization with single layers of different thicknesses. We repeat the design procedure three times for each pair of high and low index materials, every time increasing optical thickness of the starting layer so to obtain one, two, and three cluster designs. As a result we obtain six optimal AR designs, three designs with Ta_2O_5/SiO_2 and three designs with Nb_2O_5/SiO_2 thin-film materials. We shall refer to these designs as AR-Ta-1, AR-Ta-2, AR-Ta-3, and AR-Nb-1, AR-Nb-2, AR-Nb-3, respectively.

The main characteristics of the AR designs (number of layers m, TOT, and R_{av} values) are presented in Table 2. In this table we observe that the number of layers is increased by the value close to 10 from one optimal design to another. This is in agreement with estimation of $N_c = 10$ calculated above for this particular AR design problem. The average increases of TOTs are 1118 nm and 1134 nm in the cases of Ta_2O_5/SiO_2 and Nb_2O_5/SiO_2, respectively, which is again consistent with theoretical estimations calculated above.

Average residual reflectance values are decreasing from design to design in the 3rd and 8th columns of Table 2 and approaching to the minimal achievable reflectance values R_∞ calculated using expression from [14]. These values equal to 1.17% and 1.00% in the cases of Ta_2O_5/SiO_2 and Nb_2O_5/SiO_2, respectively. In Figs. 1 and 2 we show theoretical reflectance of the designed AR. It is visually observed in Figs. 1 and 2 that only insignificant decrease of residual reflectance is achieved with growing TOT and number of layers. This is confirmed numerically as well. The absolute decreases of R_{av} of two-cluster AR designs in comparison with R_{av} of one-cluster AR designs (rows 2 and 3 of Table 2) are 0.15% and 0.2% and the absolute decreases of R_{av} of three-cluster AR designs in comparison with R_{av} of two-cluster AR designs (rows 3 and 4 of Table 2) are 0.09% and 0.06%. These decreases are quite small from a practical point of view.

To check whether complication of a theoretical design is practically reasonable we analyze the sensitivity of the obtained designs to the random errors in layer thicknesses. For this purpose we apply a standard error analysis procedure [2,24]. Let M be the number of tests. We specify independent normally distributed random errors in layer thicknesses of AR design and calculate average residual reflectances of these designs $\hat{R}_{av,i}$, $i = 1, \ldots, M$. Then we calculate average deviation $E(\Delta R_{av})$:

$$E(\Delta R_{av}) = \frac{1}{M}\sum_{i=1}^{M}(\hat{R}_{av,i} - R_{av}). \quad (7)$$

The numerical values of $E(\Delta R_{av})$ calculated for three levels of root-mean square deviations of absolute errors, namely 0.5 nm, 1 nm, and 2 nm, are presented in Table 3. We provided error analysis for

Table 2. Parameters of the AR Designs for the 450 nm to 1800 nm Spectral Range

Materials: Ta_2O_5 and SiO_2				Materials: Nb_2O_5 and SiO_2			
Design Name	m	TOT, nm	R_{av}, %	Design Name	m	TOT, nm	R_{av}, %
AR-Ta-1	10	1133	1.60	AR-Nb-1	12	1100	1.44
AR-Ta-2	20	2185	1.44	AR-Nb-2	22	2283	1.24
AR-Ta-3	30	3369	1.35	AR-Nb-3	30	3368	1.19

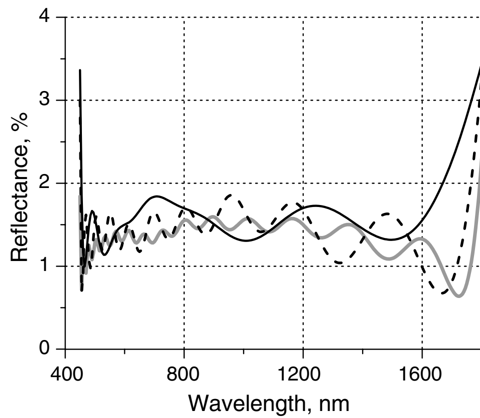

Fig. 1. Comparison of theoretical reflectance data of the designs AR-Ta-1 (solid black curve), AR-Ta-2 (dashed curve) and AR-Ta-3 (gray thick curve).

these levels of errors because they are estimations of deposition accuracy that is achieved in deposition system in our disposal. We provide more details about deposition plant and monitoring accuracy in the next sections.

We observe that $E(\Delta R_{av})$ grow with growing number of layers. The most important is that $E(\Delta R_{av})$ values of two-cluster designs AR-Ta-2 and AR-Nb-2 exceed absolute decreases of R_{av} when adding the second cluster and $E(\Delta R_{av})$ values of three-cluster designs AR-Ta-3 and AR-Nb-3 exceed absolute decreases of R_{av} when adding the third cluster for all considered values of thickness errors. This errors analysis convinces us to choose the one-cluster designs AR-Ta-1 and AR-Nb-1 for practical realization. Thicknesses of the design layers are presented in Table 4.

3. Monitoring Antireflection Coatings

We have two monitoring techniques at our disposal: broadband monitoring (BBM) and time monitoring (TM). In this section we choose the monitoring technique which is the most suitable for production of our selected AR designs. It is known that different

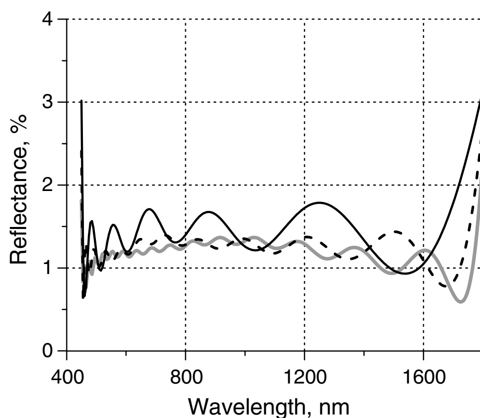

Fig. 2. Comparison of theoretical reflectance data of the designs AR-Nb-1 (solid black curve), AR-Nb-2 (dashed curve) and AR-Nb-3 (gray thick curve).

Table 3. Analysis of AR Designs Stability to Errors in Layer Thicknesses

Materials: Ta_2O_5 and SiO_2			Materials: Nb_2O_5 and SiO_2		
Design Name	Level of Errors, nm	$E(\Delta R_{av})$	Design Name	Level of Errors, nm	$E(\Delta R_{av})$
AR-Ta-1	0.5	0.12	AR-Nb-1	0.5	0.19
	1.0	0.26		1.0	0.35
	2.0	0.54		2.0	0.80
AR-Ta-2	0.5	0.23	AR-Nb-2	0.5	0.30
	1.0	0.39		1.0	0.56
	2.0	0.82		2.0	1.29
AR-Ta-3	0.5	0.32	AR-Nb-3	0.5	0.31
	1.0	0.58		1.0	0.59
	2.0	1.35		2.0	1.40

monitoring techniques give rise to deposition errors of different types [2]. In the case of BBM technique, errors in subsequent coating layers are correlated [20,25]. In the case of well-calibrated TM, errors in layer thicknesses are independent. In the present study we choose an appropriate monitoring technique on the basis of computational manufacturing experiments [19] and estimations of production yields [18].

We use special range targets specifying an allowed corridor for spectral characteristics of the simulated designs. Experiments with spectral characteristics lying inside such corridors are considered as successful ones. We estimate production yields as ratios of numbers of successful computational experiments to the total number of experiments. We denote Y (BBM) and Y(TM) production yield estimations in the cases of BBM and TM, respectively. In the course of computational experiments we model all major factors causing deposition errors [19]. We use Optilayer thin-film software [24] to perform computational manufacturing experiments.

In the course of computational manufacturing experiments we shall deal with transmittance data instead of reflectance data. In order to take into account real environment we shall also take substrate back side into account. We choose transmittance data

Table 4. Two AR Designs for the 450 nm to 1800 nm Spectral Range, Physical Thicknesses of Layers Numbered from the Substrate

Layer number	AR-Ta-1 Thicknesses, nm	AR-Ta-1 Material	AR-Nb-1 Thicknesses, nm	AR-Nb-1 Material
1	5.31	Ta_2O_5	7.93	Nb_2O_5
2	91.56	SiO_2	79.88	SiO_2
3	21.41	Ta_2O_5	24.47	Nb_2O_5
4	57.21	SiO_2	47.95	SiO_2
5	45.10	Ta_2O_5	45.92	Nb_2O_5
6	23.08	SiO_2	17.49	SiO_2
7	200.93	Ta_2O_5	115.07	Nb_2O_5
8	30.93	SiO_2	7.00	SiO_2
9	32.21	Ta_2O_5	56.64	Nb_2O_5
10	136.32	SiO_2	36.47	SiO_2
11			27.15	Nb_2O_5
12			138.21	SiO_2

because, in the real deposition process transmittance data will be recorded and after the deposition transmittance data of the produced samples will be measured and compared with theoretical transmittance.

We specify range targets as $T(\lambda_j) > T_{\mathrm{AR}}$, where $\{\lambda_j\}$ are evenly distributed points in the spectral ranges from 460 nm to 1310 nm and from 1480 nm to 1730 nm. We do not specify the range target in the spectral range from 1310 nm to 1480 nm because it is the range of water absorption of Suprasil substrates. Below we estimate production yield with various values of T_{AR}. We present only the results for the case of Ta_2O_5/SiO_2 AR because the results for Nb_2O_5/SiO_2 case are similar.

Evidently, the results of computational manufacturing experiments can be considered as reliable ones only in the case when a real deposition process is adequately simulated. Because of this reason in the course of our computational experiments we specify deposition parameters which are as close as possible to real deposition parameters. Instability of deposition rates are simulated by presenting them as stationary random processes [19] with mean values of 0.3 nm/s for Ta_2O_5 and 0.4 nm/s for SiO_2. Standard deviations of these rates from mean values are 0.05 nm/s for both materials. The correlation times are 3 s. Mean shutter delays are equal to 0.2 s.

In the case of BBM experiments monitoring data are measured in the spectral range from 400 nm to 950 nm with a wavelength step of 1 nm. Arrays of monitoring data are recorded each 1 s. Errors in measured transmittance data are presented by a random noise with a 1% level and by calibration drift of the transmittance curve as a whole with rms of 0.2%.

We performed three series of computational experiments with increasing T_{AR} values of 93%, 93.5% and 94%. According to theoretical estimations of the total number of computational experiments, which are required for reliable estimations of production yields and design selection [18], we start with 100 experiments. Estimations of production yields are presented in the second column of Table 5. We observe that yields are quite low, especially when $T_{\mathrm{AR}} = 94\%$. Probably, such low production yields are explained by presence of thin layers in optimal AR designs. We do not proceed simulations with larger numbers of experiments because as it was shown in [18] the larger numbers of experiments are required only to confirm high production yields, that is definitely not our case.

In the case of TM the errors in layer thicknesses are not correlated and we apply a standard errors analysis procedure already described in the previous section. We specify the same range targets as for the BBM case. We start with 100 computational experiments and then in order to confirm quite high production yields we perform 5000 experiments. In the course of the experiments we specify normally distributed absolute errors of 0.5 nm, 1 nm, 1.5 nm, and 2 nm rms levels. The levels in the range 1–2 nm correspond to the TM accuracy of the deposition system which we use for AR designs production and which is described in the next section. The obtained yield estimations, calculated on the basis of 5000 experiments, are presented in the last column of Table 5. The level of 0.5 nm is less than estimated monitoring accuracy but we perform computational experiments also for this level only to demonstrate that this level would provide 100% yield.

Table 5. Comparison of Design Production Yields Calculated for the Case of Broadband Monitoring (Left Side) and Time Monitoring (Right Side)

Range Target T_{AR}, %	Y(BBM), %	Level of Errors in Layer Thicknesses, nm	Y(TM), %
93	75	0.5	100
		1.0	99
		1.5	94
		2.0	81
93.5	60	0.5	100
		1.0	98
		1.5	83
		2.0	63
94	20	0.5	100
		1.0	89
		1.5	62
		2.0	34

In the worst case, when monitoring accuracy is of 2 nm level and T_{AR} is 93% the values of Y(BBM) and Y(TM) are close. In all other cases in Table 5 we observe that the TM yield values are considerably higher than the BBM yield values. This comparison is a convincing argument to use TM in the course production of our AR designs.

4. Production of Experimental Samples

In order to produce designed AR coatings we use the Leybold Optics magnetron sputtering HELIOS plant using TM of layer thicknesses [26]. In this plant, high quality dispersive mirrors with many dozens of layers were successfully deposited [26–28] and the monitoring accuracy is estimated as 1–2 nm [27,28]. Helios deposition plant is equipped also with BBM system [29]. Based on the results of the previous section we use TM to control layer thicknesses. In the course of the deposition the BBM device works in a passive mode only for data acquisition: broadband transmittance scans are recorded after deposition of each layer.

We started with experiment on the deposition of AR-Ta-1 design. We deposited two samples in one deposition run simultaneously. Our turntable has 16 sample positions, located at the same distance from the center of rotation. Exactly in the middle of two sample positions of turntable we placed a sample and a test-sample. Uniformity between different positions is better than 0.2% of layer thickness and cannot affect obtained results. The sample, denoted AR-Ta-Sup, is the design AR-Ta-1 on Suprasil substrate of 6.35 mm. The test-sample, denoted AR-Ta-glass, was placed on the position were BBM monitoring system performs measurements and it is the design

AR-Ta-1 on glass substrate B260 of 1 mm thickness. Glass B260 has a flat transmission spectrum in range above 350 nm, refractive index is specified by the Cauchy formula Eq. (1) with coefficients given in Table 1.

After the deposition, transmittance of both produced samples were measured at normal incidence in the spectral range from 325 nm to 2000 nm using a PerkinElmer LAMBDA-950 spectrophotometer. In Fig. 3 we compare measured transmittance data and theoretical transmittance data of sample AR-Ta-Sup and in Fig. 4 we compare measured transmittance data and theoretical transmittance data of sample AR-Ta-glass. In these figures excellent agreement between theoretical and experimental data is observed. We intentionally show these comparisons in different scales to demonstrate a good agreement between experimental and theoretical data in a shorter wavelength spectral range from 325 nm to 450 nm and in a longer wavelength range from 1800 nm to 2000 nm (Fig. 3) as well as coincidence of measured and theoretical transmittance oscillations in the AR spectral range (Fig. 4). In Fig. 3 we observe a water absorption peak around 1380 nm, inevitable for Suprasil substrate.

We deposited AR-Nb-1 design in the same way as we produced AR-Ta-1 design. As a result, two AR samples, AR-Nb-Sup of AR-Nb-1 design on Suprasil substrate and AR-Nb-glass of AR-Nb-1 design on glass substrate, were produced. In Fig. 5 we compare measured and theoretical transmittance data related to sample AR-Nb-Sup.

We checked that measured transmittance of AR-Ta-Sup sample in the spectral range, where range targets were specified (see Section 3), is more than 93.9% and measured transmittance of AR-Nb-Sup sample in the same range is more than 94.5%.

The achieved good agreement between experimental and theoretical transmittance data is to be considered as an indication of successful deposition of chosen AR designs.

5. Reverse Engineering of Produced AR Coatings

The main purpose to perform reverse engineering of produced AR coatings in the present study is to provide evidence that our computational experiments adequately describe the real deposition process and validate, therefore, our results and conclusions obtained on the basis of these experiments.

Although we produced AR with excellent performance, there are deviations between experimental and theoretical transmittance data. The deviations are caused by errors in layer parameters. In our experiments we used stable deposition process that produces high density films. Refractive indices of Ta_2O_5, Nb_2O_5, and SiO_2 thin-film materials deposited in Helios plant are stable and known with a high accuracy [26–28,30]. This allows us to neglect possible small offsets in layer refractive indices and determine only errors in layer thicknesses.

The measured transmittance data that we use for determination of errors in layer thicknesses is recorded by a BBM device in the course of the deposition process. A BBM device provides measurement data on a set of wavelengths $\{\lambda_j\}$, $j = 1, \ldots, L$, $L = 1239$, $\lambda_1 = 400$, $\lambda_L = 950$. Denote $d_1, \ldots, d_m$ theoretical thicknesses of considered AR designs and $\delta_1, \ldots, \delta_m$ absolute errors made in layer thicknesses. Denote $\hat{T}^{(i)}(\lambda_j)$ a measurement scan recorded after the deposition of ith layer and $T(d_1 +$

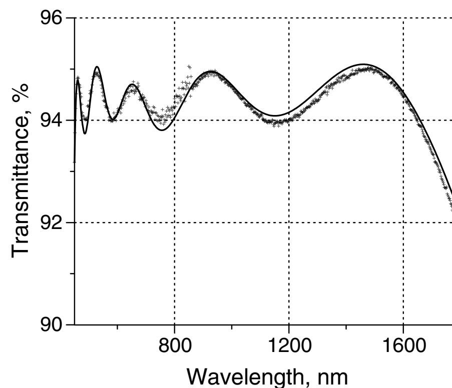

Fig. 4. Comparison of measurement transmittance data of AR-Ta-glass sample (crosses) and theoretical transmittance of the design AR-Ta-1 (solid black curve).

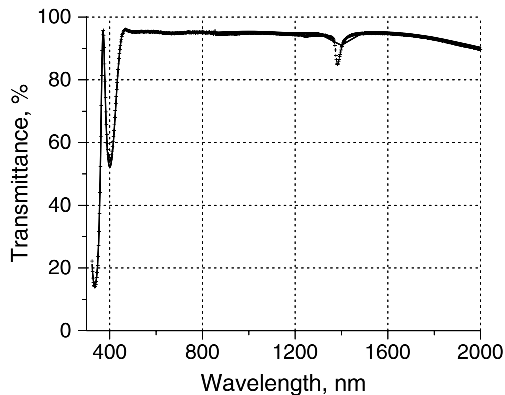

Fig. 3. Comparison of measurement transmittance data of AR-Ta-Sup sample (crosses) and theoretical transmittance of the design AR-Ta-1 (solid black curve).

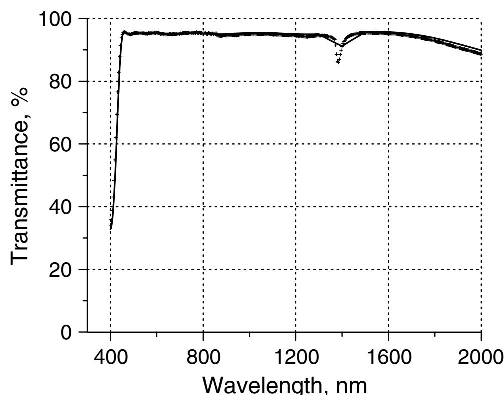

Fig. 5. Comparison of measurement transmittance data of AR-Nb-Sup sample (crosses) and theoretical transmittance of the design AR-Nb-1 (solid black curve).

$\delta_1, \ldots, d_i + \delta_i; \lambda_j)$ model transmittance data for the first i deposited coating layers.

As it has been mentioned in Section 3 a well-calibrated TM technique causes independent errors. It means that, in the course of a reverse engineering process we shall search for random errors in layer thicknesses. Generally speaking, this can be done using a well-known triangular algorithm that utilizes all multiscan measurement data [20]. This algorithm, however, cannot be applied exactly in the same way as in [20] because of the following reason. In the present study we deal with reverse engineering of AR coatings working in an ultra broadband spectral range. This spectral range includes almost entirely the BBM spectral range. In this spectral range $\hat{T}^{(i)}(\lambda)$ have only few features. In Fig. 6 the absence of oscillations and fast variations of transmittance coefficient is clearly observed. The lack of features in transmittance curves may lead to instability of solutions of reverse engineering problems in the case of AR coatings. In order to reduce this instability we use *a priori* information about smallness of errors δ_i. To take into account *a priori* information we consider a generalized discrepancy function which is obtained by adding Tikhonov's stabilizing function to the standard discrepancy function [31]:

$$\mathrm{DF}^2 = \frac{1}{Lm}\sum_{i=1}^{m}\sum_{j=1}^{L}[T(d_1+\delta_1, \ldots, d_i+\delta_i; \lambda_j) - \hat{T}^{(i)}(\lambda_j)]^2 + \alpha\sum_{i=1}^{m}\left(\frac{\delta_i}{d_i}\right)^2, \quad (8)$$

where T is measured in absolute values, and α is a so-called regularization parameter that is selected to

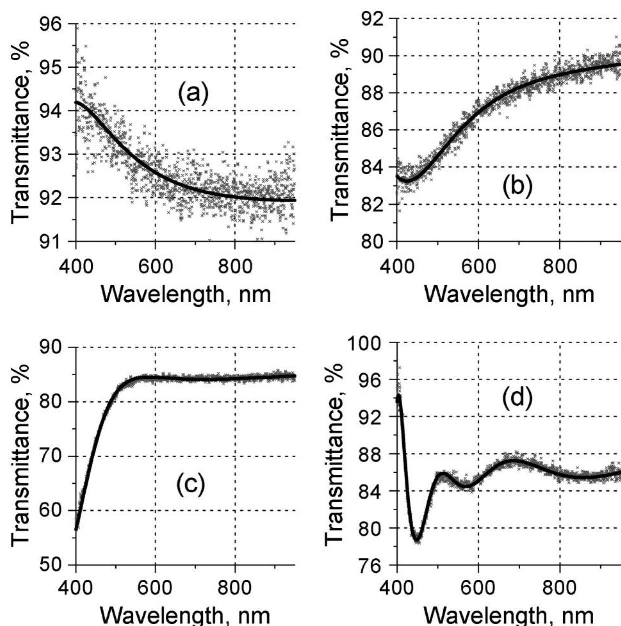

Fig. 6. Fittings of transmittance data measured after deposition of the second (a), fourth (b), sixth (c), and eighth (d) layers (crosses) by corresponding model data (solid curves).

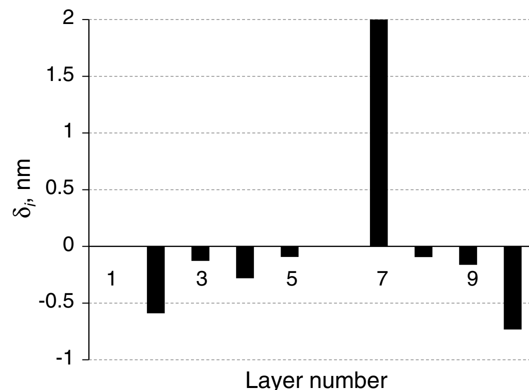

Fig. 7. Absolute errors in layer thicknesses determined on the basis of multiscan measurements related to AR-Ta-glass sample.

provide a compromise between data fitting and stability of the solution.

We perform reverse engineering of produced AR-Ta-glass and AR-Nb-glass samples because these samples were placed on the test glass position and BBM data correspond to them. Absolute errors $\delta_1, \ldots, \delta_m$ in layer thicknesses of the AR-Ta-1 sample are shown in Fig. 7. It is seen from Fig. 7 that the levels of errors in all layers except the seventh layer do not exceed 0.8 nm. The error in layer number seven is close to 2 nm. This is in a full agreement with the estimated accuracy of deposition system. In Fig. 6 we demonstrate achieved excellent fittings of transmittance data measured after the deposition of second, fourth, sixth and eighth layers, by corresponding model transmittance data. We determined also the errors in thicknesses of layers of AR-Nb-glass and found that only error in the layer number two is close to 1 nm and errors in all other layers are less than 0.5 nm.

6. Conclusions

We designed optimal two-component AR coatings for the two-octave antireflection spectral range. These designs contain thin layers which typically cause problems in the course of the deposition process. We produced these optimal AR designs in their original form without any modifications and demonstrated that it is realistic. We provided the whole design-production chain which includes: theoretical designing and selecting optimal design; choosing an appropriate monitoring technique on the basis of computational manufacturing experiments; production of AR samples using stable deposition process controlled by accurate monitoring technique; and reverse engineering of produced AR coatings. At the first, second, and last steps of this chain we used our previous theoretical results obtained in the field of AR designs as well as in the field of computational manufacturing experiments and reverse engineering algorithms. This consolidation of the theoretical results with high quality deposition facilities allowed us to obtain AR samples with excellent performance in the ultrabroadband spectral range.

This work was supported by the German Research Foundation Cluster of Excellence, Munich-Centre for Advanced Photonics (http:www.munich-photonics.de), and by the Russian Fund of Basic Research, project 10-07-00480-a (http:www.rfbr.ru).

References

1. O. Stenzel, S. Wilbrandt, and N. Kaiser, "All-oxide broadband antireflection coatings by plasma ion assisted deposition: design, simulation, manufacturing and re-optimization," Opt. Express **18**, 8704–8708 (2010).
2. H. A. Macleod, *Thin Film Optical Filters*, 3rd ed. (Institute of Physics, 2001).
3. J. Dobrowolski, "Optical properties of films and coatings," in *Optical Society of America's Handbook of Optics*, 3rd ed. (McGraw-Hill, 2010).
4. J. Dobrowolski, A. V. Tikhonravov, M. K. Trubetskov, B. T. Sullivan, and P. G. Verly, "Optimal single-band normal-incidence antireflection coatings," Appl. Opt. **35**, 644–658 (1996).
5. J. Dobrowolski, D. Paitras, P. Ma, H. Vakil, and M. Acree, "Toward perfect antireflection coatings: numerical investigation," Appl. Opt. **41**, 3075–3083 (2002).
6. U. Schulz, U. Schallenberg, and N. Kaiser, "Symmetrical periods in antireflective coatings for plastic optics," Appl. Opt. **42**, 1346–1351 (2003).
7. D. Poitras and J. Dobrowolski, "Toward perfect antireflection coatings. 2. Theory," Appl. Opt. **43**, 1286–1295 (2004).
8. J. Dobrowolski, Y. Guo, T. Tiwald, P. Ma, and D. Poitras, "Toward perfect antireflection coatings. experimental results obtained with the use of reststrahlen materials," Appl. Opt. **45**, 1555–1562 (2006).
9. U. B. Shallenberg, "Antireflection design concepts with equivalent layers," Appl. Opt. **45**, 1507–1514 (2006).
10. A. V. Tikhonravov, M. K. Trubetskov, T. V. Amotchkina, and J. A. Dobrowolski, "Estimation of the average residual reflectance of broadband antireflection coatings," Appl. Opt. **47**, C124–C130 (2007).
11. R. R. Willey, "Further guidance for broadband antireflection coating design," Appl. Opt. **50**, C274–C278 (2011).
12. T. V. Amotchkina, A. V. Tikhonravov, M. K. Trubetskov, and S. A. Yanshin, "Structural properties of antireflection coatings," in *Optical Interference Coatings*, OSA Technical Digest Series (Optical Society of America, 2007), paper WB5.
13. T. V. Amotchkina, A. V. Tikhonravov, and M. K. Trubetskov, "Estimation for the number of layers of broad band antireflection coatings," Proc. SPIE **7101**, 710104 (2008).
14. T. V. Amotchkina, "Empirical expression for the minimum residual reflectance of normal- and oblique-incidence antireflection coatings," Appl. Opt. **47**, 3109–3113 (2008).
15. U. Schulz, "Wideband antireflection coatings by combining interference multilayers with structured top layers," Opt. Express **17**, 8704–8708 (2009).
16. A. V. Tikhonravov, M. K. Trubetskov, T. V. Amotchkina, and V. Pervak, "Estimations of production yields for selection of a practical optimal optical coating design," Appl. Opt. **50**, C141–C147 (2011).
17. A. V. Tikhonravov, M. K. Trubetskov, and T. V. Amotchkina, "Computational manufacturing experiments for choosing optimal design and monitoring strategy," *Optical Interference Coatings*, OSA Technical Digest Series (Optical Society of America, 2010), paper TuA5.
18. A. V. Tikhonravov, M. K. Trubetskov, and T. V. Amotchkina, "On the reliability of computational estimations used for choosing the most manufacturable design," *Optical Interference Coatings*, OSA Technical Digest Series (Optical Society of America, 2010), paper TuA3.
19. A. V. Tikhonravov and M. K. Trubetskov, "Computational manufacturing as a bridge between design and production," Appl. Opt. **44**, 6877–6884 (2005).
20. T. V. Amotchkina, M. K. Trubetskov, S. Schlichting, H. Ehlers, D. Ristau, and A. V. Tikhonravov, "Comparison of algorithms used for optical characterization of multilayer optical coatings," Appl. Opt. **50**, 3389–3395 (2011).
21. Quartz Glass for Optics: Data and Properties, http://heraeus-quarzglas.com.
22. A. V. Tikhonravov, M. K. Trubetskov, T. V. Amotchkina, and M. A. Kokarev, "Key role of the coating total optical thickness in solving design problems," Proc. SPIE **5250**, 312–321 (2004).
23. T. V. Amotchkina, "Analytical properties of the spectral characteristics of antireflection coatings," Moscow University Physics Bulletin **62**, 292–295 (2007).
24. A. V. Tikhonravov and M. K. Trubetskov, "OptiLayer thin film software," http://www.optilayer.com.
25. A. V. Tikhonravov, M. K. Trubetskov, and T. V. Amotchkina, "Investigation of the error self-compensation effect associated with broadband optical monitoring," Appl. Opt. **50**, C111–C116 (2011).
26. V. Pervak, A. V. Tikhonravov, M. K. Trubetskov, S. Naumov, F. Krausz, and A. Apolonski, "1.5-octave chirped mirror for pulse compression down to sub-3 fs," Appl. Phys. B **87**, 5–12 (2006).
27. V. Pervak, M. K. Trubetskov, and A. V. Tikhonravov, "Robust synthesis of dispersive mirrors," Opt. Express **19**, 2371–2380 (2011).
28. V. Pervak, "Recent developments and new ideas in the field of dispersive multilayer optics," Appl. Opt. **50**, C55–C61 (2011).
29. D. Ristau, H. Ehlers, T. Gross, and M. Lappschies, "Optical broadband monitoring of conventional and ion processes," Appl. Opt. **45**, 1495–1501 (2006).
30. A. V. Tikhonravov, M. K. Trubetskov, T. V. Amotchkina, G. DeBell, V. Pervak, A. K. Sytchkova, M. Grilli, and D. Ristau, "Optical parameters of oxide films typically used in optical coating production," Appl. Opt. **50**, C75–C85 (2011).
31. A. N. Tikhonov and V. Y. Arsenin, *Solutions of Ill-Posed Problems* (Wiley, 1977).